J Therm Anal Calorim (2010) 100:981–985
DOI 10.1007/s10973-009-0402-z

Synthesis and thermal stability of hydrotalcites containing manganese

Laure-Marie Grand · Sara J. Palmer · Ray L. Frost

Received: 31 May 2009 / Accepted: 29 July 2009 / Published online: 28 August 2009

Abstract The hydrotalcite based upon manganese known as charmarite $Mn_4Al_2(OH)_{12}CO_3 \cdot 3H_2O$ has been synthesised with different Mn/Al ratios from 4:1 to 2:1. Impurities of manganese oxide, rhodochrosite and bayerite at low concentrations were also produced during the synthesis. The thermal stability of charmarite was investigated using thermogravimetry. The manganese hydrotalcite decomposed in stages with mass loss steps at 211, 305 and 793 °C. The product of the thermal decomposition was amorphous material mixed with manganese oxide. A comparison is made with the thermal decomposition of the Mg/Al hydrotalcite. It is concluded that the synthetic charmarite is slightly less stable than hydrotalcite.

Keywords Charmarite · Rhodochrosite · Hydrotalcite · Hydrocalumite · Synthesis · Thermal stability

Introduction

Hydrotalcites have been known for an extended period of time [1–3]. Hydrotalcites, or layered double hydroxides (LDH) are fundamentally known as anionic clays [4]. Hydrotalcites containing manganese are known [5–8]. The natural mineral is known as charmarite [9]. The application of hydrotalcites containing manganese rests with their application in catalyst science [7, 10–15]. Some of these types of materials are used for adsorption and chemical storage [8, 16, 17]. However the synthesis and characterization of hydrotalcites containing manganese remains unexplored and not studied.

Hydrotalcites consist of stacked layers of metal cations (M^{2+} and M^{3+}) similar to brucite ($Mg(OH)_2$). The structure of hydrotalcite can be derived from a brucite structure ($Mg(OH)_2$) in which e.g. Al^{3+} or Fe^{3+} (pyroaurite-sjögrenite) substitutes a part of the Mg^{2+} [2, 18–20]. This substitution creates a positive layer charge on the hydroxide layers, which is compensated by interlayer anions or anionic complexes. In general any divalent cation could substitute for the Mg^{2+} in the brucite-like layer, including Mn^{2+}. Hydrotalcites consist of stacked layers of metal cations (M^{2+} and M^{3+}) similar to brucite ($Mg(OH)_2$). For hydrotalcite-like structures, the substitution of divalent cations for trivalent ones (of similar radii), gives rise to a positive charge on the brucite-like layers. In hydrotalcites a broad range of compositions are possible of the type $\left[M^{2+}{}_{1-x}M^{3+}{}_{x}(OH)_2\right]_{x/n} \cdot yH_2O$, where M^{2+} and M^{3+} are the di- and tri-valent cations in the octahedral positions within the hydroxide layers with x normally between 0.17 and 0.33. A^{n-} is an exchangeable interlayer anion [21]. The positively charged hydroxyl layers are neutralised through the intercalation and adsorption of anionic species, therefore stabilising the structure. Anions that are intercalated between the hydroxyl layers need to meet certain criteria, including having a high charge density and small anionic radius.

This study is focused upon the synthesis, characterisation of hydrotalcites with manganese substituting for magnesium in the brucite layer of hydrotalcites.

L.-M. Grand · S. J. Palmer · R. L. Frost (✉)
Inorganic Materials Research Program, School of Physical and Chemical Sciences, Queensland University of Technology, GPO Box 2434, Brisbane, Queensland 4001, Australia
e-mail: r.frost@qut.edu.au

L.-M. Grand
ENSICAEN, 6 Boulevard Marechal Juin, 14050 Caen Cedex 4, France

Experimental

Synthesis of hydrotalcite samples

The hydrotalcites were synthesised by the co-precipitation method using analytical grade chemicals. Two solutions were prepared, solution 1 contained 2 M NaOH and 0.2 M Na_2CO_3, and solution 2 contained Mn^{2+} ($MnCl_2 \cdot 4H_2O$) at different concentrations, together with Al^{3+} ($AlCl_3 \cdot 6H_2O$). Solution 2 was added at a steady rate to solution 1 drop wise, under vigorous stirring. A separating funnel was used to deliver solution 2 to solution 1. The precipitated minerals were washed at ambient temperatures thoroughly with ultra pure water to remove any residual salts and dried in an oven (85 °C) overnight. Table 1 shows the masses and concentrations used to synthesise hydrotalcites with a range of Mn/Al ratios.

Characterisation techniques

Thermal decomposition of approximately 50 mg of hydrotalcite was carried out in a TA® Instruments incorporated high-resolution thermogravimetric analyser (series Q500) in a flowing nitrogen atmosphere (80 cm^3/min), at a rate of 2.0 °C/min up to 1000 °C. X-ray diffraction patterns were collected using a Philips X'pert wide angle X-ray diffractometer, operating in step scan mode, with Cu Kα radiation (1.54052 Å). For more information on the experimental and analysis techniques used, refer to previous work by the authors [22–27].

Results and discussion

X-ray diffraction

The powdered XRD patterns of the synthesised manganese hydrotalcites together with probable impurities are shown in Fig. 1. The natural mineral is known as charmarite $Mn_4Al_2(OH)_{12}CO_3 \cdot 3H_2O$ [9, 28] and the XRD pattern of this mineral is shown in Fig. 1. The XRD patterns show that the compound equivalent to the mineral charmarite has been successfully synthesised over a range of concentrations from 4:1 Mn/Al to 2:1. Some impurities are observed in the synthesised manganese hydrotalcite including manganese oxide (Mn_3O_4), bayerite and rhodochrosite ($MnCO_3$). The formation of Mn/Al hydrotalcites, under these specific synthesis conditions, does not appear to be the most favourable reaction, especially as the concentration of manganese increases in solution. It is proposed that the increase in cation size, compared to magnesium hydrotalcites, restricts the formation of hydrotalcite and allows for other manganese phases to form. It is observed that manganese oxide (predominate phase) and rhodochrosite form predominantly in high manganese concentrations. The d(003) spacing varies from 7.70 Å to 7.79 Å. It is concluded that the hydrotalcite based upon divalent manganese is successfully synthesised over a wide range of Mn/Al ratios. It should be noted that sodium chloride is not a true precipitate that forms, it is present due to the drying process.

Table 1 Masses and concentrations for the synthesis of manganese containing hydrotalcites with various Mn/Al ratios

Mn/Al ratio	2:1	2.5:1	3:1	3.5:1	4:1
Concentration of $MnCl_2 \cdot 4H_2O$	0.67 M	0.71 M	0.75 M	0.77 M	0.80 M
Masses of $MnCl_2 \cdot 4H_2O$	6.63 g	7.02 g	7.42 g	7.62 g	7.92 g
Concentration of $AlCl_3 \cdot 6H_2O$	0.33 M	0.29 M	0.25 M	0.22 M	0.20 M
Masses of $AlCl_3 \cdot 6H_2O$	3.98 g	3.45 g	3.02 g	2.68 g	2.41 g

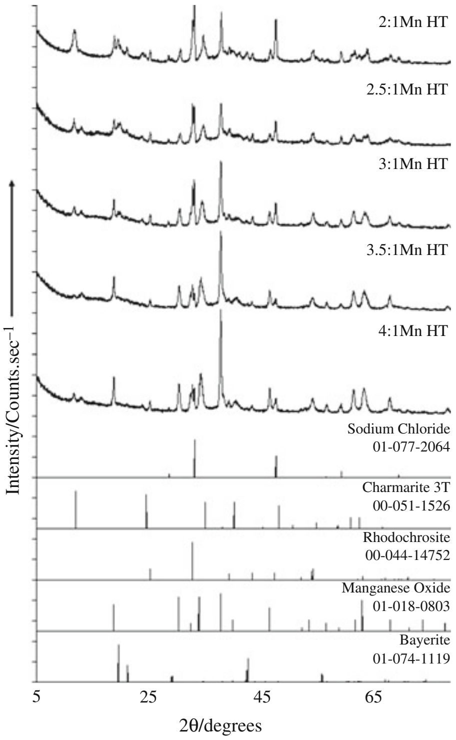

Fig. 1 Powder X-ray diffraction of the synthesised manganese hydrotalcites in the 2:1 to 4:1 ratio

A comparison may be made with the d-spacings of natural hydrotalcites. There exists in nature a significant number of hydrotalcites which are formed as deposits from ground water containing Ni^{2+} and Fe^{3+} [29]. These are based upon the dissolution of Ni–Fe sulphides during weathering. Normally the hydrotalcite structure based upon takovite (Ni, Al) and hydrotalcite (Mg, Al) have basal spacings of ~8.0 Å, where the interlayer anion is carbonate. If the carbonate anion is replaced by sulphate, then the mineral carrboydite is obtained. Similarly reevesite is the (Ni, Fe) hydrotalcite with carbonate as the interlayer anion, which when replaced by sulphate the minerals honessite and hydrohonessite are obtained. Among the naturally occurring hydrotalcites are carrboydite and hydrohonessite [30, 31]. These two hydrotalcites are based upon the incorporation of sulphate into the interlayer with expansions of 10.34–10.8 Å.

Thermal analysis—TG and DTG

The TG and DTG curves for the thermal decomposition of the synthesised charmarite are displayed in Fig. 2. The DTG curve of the manganese hydrotalcite resembles those observed for magnesium hydortalcites, Fig. 3. The main difference between these different hydrotalcites is the stability of the interlayer water within the hydrotalcite structure. However, the three main decomposition steps observed for magnesium hydrotalcite structures are observed in the manganese hydortalcite: (1) removal of adsorbed water, (2) removal of interlayer water, (3) dehydroxylation and decarbonation of the hydrotalcite structure.

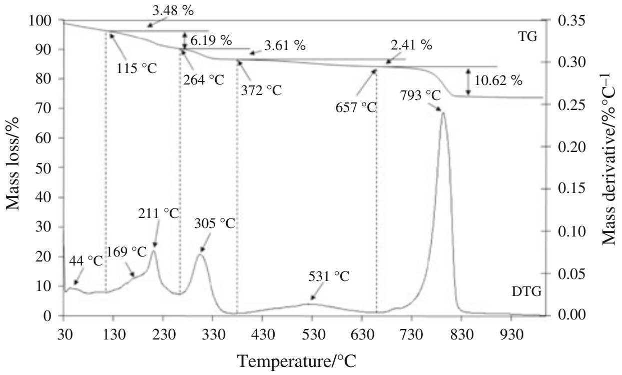

Fig. 2 TG and DTG curve of the 3:1 Mn^{2+}/Al^{3+} hydrotalcite

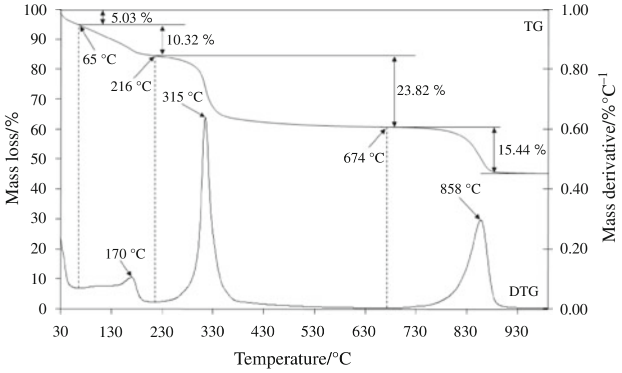

Fig. 3 TG and DTG curve of the 3:1 Mg^{2+}/Al^{3+} hydrotalcite

A series of TG steps are observed with maxima in the DTG curves at 44, 169, 211, 305, 531 and 793 °C. The first mass loss at 44 °C is ascribed to the loss of adsorbed water. The theoretical formula based on the molar ratio of Mn^{2+} and Al^{3+} in solution is $Mn_6Al_2(OH)_{16}CO_3{\cdot}4H_2O$. The number of moles of water associated with the structure has been calculated from the theoretical formula and the combined mass loss between 0 and 260 °C, Appendix. The broad mass loss, ranging from 115 °C to 264 °C, is attributed to the loss of water in the interlayer region. The total mass loss for these two steps is 9.67% (respectively 3.48 and 6.19%). Compared to the mass losses at higher temperatures, a considerable amount of adsorbed water is associated with this structure. The following thermal decomposition is proposed for the removal of water:

$$Mn_6Al_2(OH)_{16}CO_3{\cdot}4H_2O \rightarrow Mn_6Al_2(OH)_{16}CO_3 + 4H_2O$$

The decomposition of the hydroxyl layers of the HT structure occurs as a broad peak centred at around 305 °C. The OH units of the brucite-like layers decompose to its corresponding oxides, shown by the decomposition equation below:

$$\begin{aligned}3Mn_6Al_2(OH)_{16}CO_3 \rightarrow\ & 5Mn_3O_4 + 3CO_2 + 3MnAl_2O_4 \\ & + 16H_2O + 3/2O_2\end{aligned}$$

The peak at 531 °C is assigned to the decomposition of $MnCO_3$. A mass loss of 2.41% is observed, ($MnCO_3 \rightarrow MnO + CO_2$). XRD did not find MnO in the TG residue,

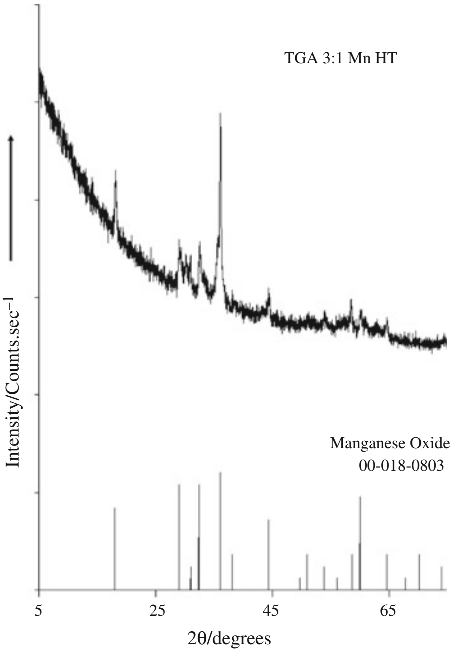

Fig. 4 XRD of the products of the thermal decomposition of manganese containing hydrotalcite

however, due to the small concentration of this phase it is proposed XRD is not sensitive enough to detect this phase.

A higher temperature mass loss at around 793 °C of 10.62% is observed and is assigned to the decomposition of the residual salt. The XRD of the product of the thermal decomposition of charmarite is provided in Fig. 4. The product shows a great deal of amorphicity. The main product according to the XRD is manganese oxide.

Conclusions

The hydrotalcite mineral charmarite with different Mn/Al ratios have been successfully synthesised. Manganese hydrotalcite thermally decomposes in stages with mass loss steps at 170 °C attributed to water loss, and at 315 °C assigned to the loss of carbonate and OH units. The impurity $MnCO_3$ is proposed to decompose between 400 and 660 °C to CO_2 and manganese oxide. The thermal analysis of the residue showed all compounds decomposed to manganese oxide. The synthesised charmarite also thermally decomposes in steps with principal peaks in the DTG curve at 169, 211 and 305 °C, corresponding well to the decomposition of magnesium hydrotalcites. It is concluded that the thermal stability of charmarite is similar to but slightly less stable than magnesium hydrotalcites.

Acknowledgements The financial and infra-structure support of the Queensland Research and Development Centre (QRDC-RioTintoAlcan) and the Queensland University of Technology Inorganic Materials Research Program of the School of Physical and Chemical Sciences are gratefully acknowledged. One of the authors (LMG) thanks the Queensland University of Technology for a visiting student fellowship.

Appendix

Calculation of water content for Mn^{2+}/Al^{3+} hydrotalcite

Proposed composition $Mn_6Al_2(OH)_{16}CO_3{\cdot}xH_2O$
Total mass of hydrotalcite analysed: 26.852 mg
% mass loss of water up to 264 °C: 9.67%
Mass of water removed up to 264 °C: 2.5966 mg
Molar mass of water: 18.02 g mol^{-1}
Moles of water removed: 0.144095 mmol
Mass of dehydrated mineral: 26.852 – 2.5966 = 24.2554 mg
Molar mass of dehydrated mineral: 715.738 g mol^{-1}
Moles of dehydrated mineral: 0.033888 mmol

Calculation of x:

1 mol dehydrated mineral: x mol H_2O
0.033888 mmol dehydrated mineral: 0.144095 mmol H_2O
$x = 4.2521 - 4$ mol
Formula: $Mn_6Al_2(OH)_{16}CO_3{\cdot}4H_2O$

References

1. Allmann R. Crystal structure of pyroaurite. Acta Crystallogr. 1968;24:972–7.
2. Ingram L, Taylor HFW. Crystal structures of sjoegrenite and pyroaurite. Mineral Mag. 1967;36:465–79.
3. Taylor HFW. Crystal structures of some double hydroxide minerals. Mineral Mag. 1973;39:377–89.
4. Rives V, editor. Layered double hydroxides: present and future. New York: Nova Science Publishers, Inc.; 2001.
5. Boclair JW, Braterman PS. Layered double hydroxide stability. 1. Relative stabilities of layered double hydroxides and their simple counterparts. Chem Mater. 1999;11:298–302.
6. Chen H-q, Zhan Z-k. Synthesis, characterization and catalysis of Cu–Mn–Al hydrotalcite like compounds, Huaxue Yanjiu Yu Yingyong 2007;19:877–81.
7. Fernandez JM, Barriga C, Ulibarri M-A, Labajos FM, Rives V. Preparation and thermal stability of manganese-containing hydrotalcite. J Math Chem. 1994;4:1117–21.
8. Sampieri A, Fetter G, Pfeiffer H, Bosch P. Carbonate phobic (Zn, Mn)-Al hydrotalcite-like compounds. Solid State Sci. 2007;9: 394–403.
9. Chao GY, Gault RA. Quintinite-2H, quintinite-3T, charmarite-2H, charmarite-3T and caresite-3T, a new group of carbonate minerals related to the hydrotalcite—manasseite group. Can Mineral. 1997;35:1541–9.
10. Chen A, Xu H, Le Y, Hua W, Shen W, Gao Z. Catalyst using M/Mn/Al hydrotalcite as precursor and its preparation process. Fudan University, People Report China. Application: CN CN; 2004, p. 11.
11. Chen A, Xu H, Yue Y, Shen W, Hua W, Gao Z. M-Mn-Al Hydrotalcite-like Compounds as Precursors for Methyl Benzoate Hydrogenation Catalysts. Ind Eng Chem Res. 2004;43:6409–15.
12. Cheng H, Ding W, Lu X, Zhang Y, Ai X. Hydrotalcite type hydrocracking catalyst and its preparation method. Shanghai University, People Report China. Application: CN CN; 2008, p. 8.
13. Ebitani K, Motokura K, Mizugaki T, Kaneda K. Heterotrimetallic RuMnMn species on a hydrotalcite surface as highly efficient heterogeneous catalysts for liquid-phase oxidation of alcohols with molecular oxygen. Angew Chem Int Ed. 2005;44:3423–6.
14. Jiratova K, Cuba P, Kovanda F, Hilaire L, Pitchon V. Preparation and characterisation of activated Ni (Mn)/Mg/Al hydrotalcites for combustion catalysis. Catal Today. 2002;76:43–53.
15. Pacultova K, Obalova L, Kovanda F, Jiratova K. Catalytic reduction of nitrous oxide with carbon monoxide over calcined Co-Mn-Al hydrotalcite. Catal Today. 2008;137:385–9.
16. Chitrakar R, Tezuka S, Sonoda A, Sakane K, Ooi K, Hirotsu T. Adsorption of phosphate from seawater on calcined MgMn-layered double hydroxides. J Colloid Interface Sci. 2005;290:45–51.
17. Harrison DP. Sorption-enhanced hydrogen production: a review. Ind Eng Chem Res. 2008;47:6486–501.

18. Brown G, Van Oosterwyck-Gastuche MC. Mixed magnesium-aluminum hydroxides. II. Structure and structural chemistry of synthetic hydroxycarbonates and related minerals and compounds. Clay Miner. 1967;7:193–201.
19. Taylor HFW. Segregation and cation-ordering in sjogrenite and pyroaurite. Mineral Mag. 1969;37:338–42.
20. Taylor RM. Stabilization of color and structure in the pyroaurite-type compounds iron(II) iron(III) aluminum(III) hydroxycarbonates. Clay Miner. 1982;17:369–72.
21. Kloprogge JT, Wharton D, Hickey L, Frost RL. Infrared and Raman study of interlayer anions CO2–3, NO-3, SO2–4 and ClO-4 in Mg/Al-hydrotalcite. Am Mineral. 2002;87:623–9.
22. Frost RL, Hales MC, Martens WN. Thermogravimetric analysis of selected group (II) carbonate minerals—Implication for the geosequestration of greenhouse gases. J Therm Anal Calorim. 2009;95:999–1005.
23. Palmer SJ, Spratt HJ, Frost RL. Thermal decomposition of hydrotalcites with variable cationic ratios. J Therm Anal Calorim. 2009;95:123–9.
24. Frost RL, Locke AJ, Hales MC, Martens WN. Thermal stability of synthetic aurichalcite. Implications for making mixed metal oxides for use as catalysts. J Therm Anal Calorim. 2008;94:203–8.
25. Vagvoelgyi V, Daniel LM, Pinto C, Kristof J, Frost RL, Horvath E. Dynamic and controlled rate thermal analysis of attapulgite. J Therm Anal Calorim. 2008;92:589–94.
26. Vagvolgyi V, Frost RL, Hales M, Locke A, Kristof J, Horvath E. Controlled rate thermal analysis of hydromagnesite. J Therm Anal Calorim. 2008;92:893–7.
27. Vagvolgyi V, Hales M, Martens W, Kristof J, Horvath E, Frost RL. Dynamic and controlled rate thermal analysis of hydrozincite and smithsonite. J Therm Anal Calorim. 2008;92:911–6.
28. Pagano R. New minerals. Updates of systematic mineralogy, Rivista Mineralogica Italiana 1999;1:62–6.
29. Nickel EH, Wildman JE. Hydrohonessite—a new hydrated nickel-iron hydroxysulfate mineral; its relationship to honessite, carrboydite, and minerals of the pyroaurite group. Mineral Mag. 1981;44:333–7.
30. Bish DL, Livingstone A. The crystal chemistry and paragenesis of honessite and hydrohonessite: the sulfate analogs of reevesite. Mineral Mag. 1981;44:339–43.
31. Nickel EH, Clarke RM. Carrboydite, a hydrated sulfate of nickel and aluminum: a new mineral from Western Australia. Am Mineral. 1976;61:366–72.